ELSEVIER

Journal of Nuclear Materials 297 (2001) 35–42

journal of nuclear materials

www.elsevier.com/locate/jnucmat

Coarsening-densification transition temperature in sintering of uranium dioxide

Palanki Balakrishna *, B. Narasimha Murty, K.P. Chakraborthy, R.N. Jayaraj, C. Ganguly

Nuclear Fuel Complex, Hyderabad 500 062, India

Received 12 December 2000; accepted 12 April 2001

Abstract

The concept of coarsening–densification transition temperature (CDTT) has been proposed to explain the experimental observations of the study of sintering undoped uranium dioxide and niobia-doped uranium dioxide powder compacts in argon atmosphere in a laboratory tubular furnace. The general method for deducing CDTT for a given material under the prevailing conditions of sintering and the likely variables that influence the CDTT are described. Though the present work is specific in nature for uranium dioxide sintering in argon atmosphere, the concept of CDTT is fairly general and must be applicable to sintering of any material and has immense potential to offer advantages in designing and/or optimizing the profile of a sintering furnace, in the diagnosis of the fault in the process conditions of sintering, and so on. The problems of viewing the effect of heating rate only in terms of densification are brought out in the light of observing the undesirable phenomena of coring and bloating and causes were identified and remedial measures suggested.

1. Introduction

The densification behavior of a ceramic powder compact depends on the starting powder characteristics, pressing conditions and sintering conditions [1–8]. The microstructure of a ceramic is directly dependent on the temperature versus time sintering cycle definition. The microstructure evolution (which influences the course of densification) is the result of the different transport mechanisms, some of which are efficient at low temperatures while others need high temperatures [9]. In addition, uniformity and homogeneity of particle packing in the green body has an enormous impact on how well the green body will densify during sintering [10]. Different particle size distributions lead to different green and sintered microstructures. The compact inhomogeneity induces nonuniform sintering rates, which, in turn, create transient (and some times, residual) stresses which affect microstructural development [11–15].

Nuclear-grade UO_2 powders are prepared, pressed and sintered to yield pellets of high density and homogeneous microstructure as per details given elsewhere [16–19]. In the course of UO_2 pellet production, however, it was noticed that UO_2 green pellets from the same powder lot and which have seen the same processing conditions gave rise to different sintered densities when passed through different pusher-type continuous sintering furnaces. The differences in the furnaces were found to be mainly in the heating rates. Hence an attempt was made to determine the effect of heating rate on densification and other associated effects in the sintering process.

Manzel and Dorr [20] found the sintering shrinkage rate in hydrogen to be maximum at 1250°C for UO_2. According to Runfors [21], the shrinkage rate was maximum at 1250°C for UO_2 made by reduction of U_3O_8 at 630°C. This maximum shrinkage rate temperature increased to 1500°C as the reduction temperature was increased to 900°C. In a study on the initial stage sintering kinetics of UO_2, Woolfrey [22] found

* Corresponding author. Tel.: +91-40 712 0151; fax: +91-40 712 1305.

E-mail address: pbk@nfc.ernet.in (P. Balakrishna).

0022-3115/01/$ - see front matter
PII: S0022-3115(01)00599-2

that complicating factors reduced the rate of sintering below 900°C. For the same green microstructure, different sintered microstructures can result depending on the heating rate [23]. Chu et al. [24] reported that pretreatment of a green compact at a low temperature without densification produced a compact with a more uniform microstructure than the initial one. Sato and Carry [25] pointed out that pretreatments have the possibility to retard the onset of abnormal grain growth by creating a more uniform microstructure before densification begins. There are conflicting evidences on the effect of heating rate on the densification behavior of different materials where one is favored by the slower rate of heating [26] but the other by the fast firing [27]. Searcy and Beruto [28] stated that temperature gradients significantly influence the microstructural changes that occur during the firing of ceramic objects.

In this paper, the results of an investigation of the effect of heating rate and pretreatment on the densification behavior of UO_2 in argon atmosphere are presented. The term coarsening is normally used in connection with slowing down of densification in the final stage of sintering caused by grain growth and delinking of pores from grain boundaries [2,8]. Coarsening can also be used in another sense, where the internal specific surface area of a powder compact decreases without causing densification, in the first stage of sintering. It is in the latter sense that the term is used in this paper. Evidence of void coarsening is available in porosimetry curves [29].

2. Experimental

2.1. Low-temperature sintering without additive

UO_2 powder compacts from the same powder lot were sintered at 1300°C in IOLAR Grade I argon atmosphere using the heating rates 100, 300 and 600°C h^{-1} in an experimental furnace (Labin Scientific Instruments, New Delhi) where the muffle tube is made of thermal recrystallized alumina, OD 36.1 mm, ID 28.9 mm, length 60 cm. There was an inner mullite tube of diameter 30 mm and wall thickness 0.3 mm, 100 cm long. Flow of argon was maintained at 250 l h^{-1}. The cooling rate was maintained at 200°C h^{-1} in all the cases. The powder characteristics and pressing conditions are given in Table 1. The experimental set-up is shown in Fig. 1. The green densities of the pellets were in the range 5.5–5.6 g cm^{-3}. The experiment was repeated for the heating rate of 300 and 600°C h^{-1} this time, with a presoaking period of 3 h at 900°C, 1000°C and 1100°C, before final sintering at 1300°C.

Table 1
UO_2 powder and pressing characteristics

Powder precursor	Ammonium diuranate
Specific surface area (BET) (m^2 g^{-1})	3.22
Average particle size (FSSS) (μm)	2.3
Bulk density (g cm^{-3})	1.4
Tap density (g cm^{-3})	2.5
Admixed lubricant	Zinc stearate
Pressing pressure (MPa)	250
Green density (g cm^{-3})	5.5–5.6

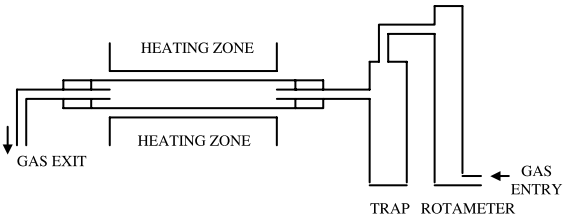

Fig. 1. Experimental low-temperature sintering set-up (schematic).

2.2. Low-temperature sintering with niobia additive

Nb_2O_5 powder was mixed with UO_2 powder (0.5 wt% Nb_2O_5) using a mortar and pestle. To ensure complete homogeneity initially 10% niobia-mixed powder was made and on further suitable dilution with fresh uranium dioxide 0.5 wt% Nb_2O_5 was made. The mixture was pelletized as before and sintered at 1300°C for 3 h, using the heating rate of 600°C h^{-1}, with and without presoaking at 900°C, 1000°C and 1100°C.

2.3. High-temperature sintering

UO_2 powder compacts from the same powder lot were sintered using two sintering furnace profiles in a pusher-type industrial sintering furnace. One is normal profile, called profile N, where the temperatures in successive heating zones were such that, for a given pushing interval, a heating rate of about 200°C h^{-1} was obtained. In contrast, in the other profile S, the temperatures were brought down so that a heating rate of about 100°C h^{-1} was obtained. The same lot of UO_2 pellets were separately subjected to profiles N and S. All the compacts were resintered using relatively faster (in comparison with profile S) heating profile N.

Quantity of charge of UO_2: The usual charge quantity in the furnace was 12 kg. Two different quantities of charge, one with the usual 12 kg and the other with 24 kg, were simultaneously subjected to profiles N and S.

3. Results

The history of the uranium dioxide used in the present study, some characteristics and pressing conditions employed are shown in Table 1.

3.1. Low-temperature sintering without additive

The sintered densities of UO_2 without additive, obtained using different heating rates to reach 1300°C are given in Table 2. Of the three heating rates employed, higher sintered density was obtained at the higher heating rates. The sintered densities of UO_2 without additive obtained with and without presoaking are shown in Table 3.

Table 2
Effect of heating rate on sintered density of UO_2

Heating rate (°C h^{-1})	100	300	600
Soaking temperature (°C)	1300	1300	1300
Soaking time (h)	3	3	3
Sintered density (g cm^{-3})	9.29	9.90	9.96

Table 3
Effect of presoaking on sintered density (g cm^{-3}) of UO_2 without niobia

Presoaking at 900°C	No presoaking	Presoaking at 1100°C
9.25	9.96	10.13

Green density: 5.5–5.6 g cm^{-3}, heating rate: 600°C h^{-1}, presoaking time: 3 h, final soaking temperature: 1300°C, final soaking time: 3 h.

Table 4
Effect of presoaking on sintered density (g cm^{-3}) of niobia-added UO_2

Presoaking at 900°C	No presoaking	Presoaking at 1100°C
10.10	10.47	10.53

Presoaking time: 3 h, final soaking temperature: 1300°C, final soaking time: 3 h.

3.2. Low-temperature sintering with niobia additive

The sintered densities of UO_2 with additive (0.5 wt% Nb_2O_5), obtained with and without presoaking are given in Table 4.

3.3. High-temperature sintering

The results are given in Table 5, where the average sintered density of 13 pellets from each boat is given for N and S sintering cycles. The table also gives the sintered densities obtained on resintering in the N cycle. The purpose of the resintering is to bring out or enlarge the effects that are not clearly visible on first sintering.

As shown in Table 5, after the first sintering cycle, there is no significant difference in the average of sintered densities with profile S and profile N. On resintering, however, the pellets that experienced the slow cycle initially, gave lower sintered densities than those which went through the cycle N. The same type of green pellets sintered differently in N + N and S + N cycles, bringing out the adverse effect of the slow cycle on densification.

Some UO_2 powder compacts exhibited coring when sintered under the N profile. Other compacts of the same powder lot were free from coring when sintered under the S profile.

Some UO_2 powder compacts exhibited bloating when the quantity of pellets was more (24 kg) under profile N, while none of the compacts showed this phenomenon when the charge was less (12 kg). On the other hand, there was no bloating in the larger charge of 24 kg when the pellets were subjected to profile S.

4. Discussion

4.1. Effect of heating rate on densification

The results show that faster heating rates favor densification. When two spheres (representing particles) are in contact the centers approach each other for volume diffusion, or grain boundary diffusion, causing densification (Fig. 2). Where there is surface diffusion or

Table 5
Sintered densities (g cm^{-3}) in slow and normal sintering cycles

S. No.	N	S	Difference	N + N	S + N	Difference
1	10.498	10.477	0.021	10.610	10.583	0.027
2	10.496	10.538	−0.042	10.533	10.383	0.150
3	10.499	10.512	−0.013	10.567	10.403	0.164
4	10.474	10.421	0.053	10.590	10.550	0.040
5	10.484	10.491	−0.007	10.537	10.533	0.004
Average	10.490	10.488	0.002	10.567	10.490	0.077
% TD	95.71	95.69	0.02	96.41	95.71	0.70

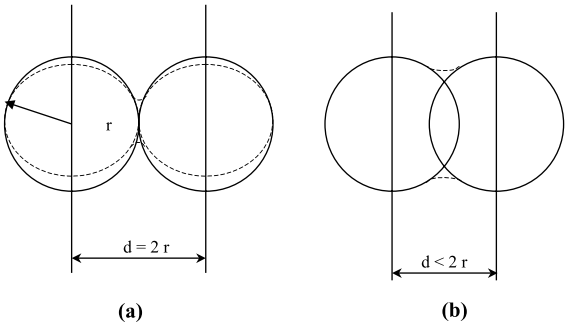

Fig. 2. Neck growth: (a) without shrinkage; (b) with shrinkage [30].

vapor transport, the centers do not approach each other and there is no densification [30]. Bulk diffusion is dominant at higher temperatures. In UO_2, cation diffusion, being slower, is rate limiting. According to Matzke [31], the cation volume diffusion coefficient is given by

$$D_{\text{vol}} = 6.5 \times 10^{-5} \exp(-129\,000/RT)\ \text{m}^2/\text{s}. \quad (1)$$

Surface diffusion is dominant at lower temperatures. The cation surface diffusion coefficient is given by

$$D_{\text{sur}} = 50 \exp(-108\,000/RT)\ \text{m}^2/\text{s}. \quad (2)$$

It is seen from the above that surface diffusion is many orders of magnitude faster than bulk diffusion and the activation energy also is lower. The diffusion coefficients are very much larger when the UO_2 is doped with Nb_2O_5 [32]. Burke et al. [33] stated that several atomic transport processes may operate simultaneously during sintering of crystalline solids. Surface to surface transport brings about growth of some crystallites at the expense of others. Such coarsening of the structure (Ostwald ripening) proceeds at constant volume fraction and is manifested by the reduction of internal surface area. Grain boundary to surface transport results in densification and is manifested by simultaneous surface area and pore volume reduction. The sintering of real compacts of fine powders is described by curves in between the two extremes, which is the result of contribution from both modes of atomic transport (Fig. 3). The more convex the trajectory of the curve (with respect to the density axis) the larger is the contribution of coarsening.

During coarsening, there is reduction in surface area without increase in density, whereas, in densification, the same is accompanied by an increase in density. If the compact is subjected to fast heating and brought to high temperature, densification takes place as surface area decreases. By going through coarsening temperature range at a fast heating rate, the surface energy is conserved initially, to be available for densification at a higher temperature. Long residence time at low temperatures seems to favor coarsening.

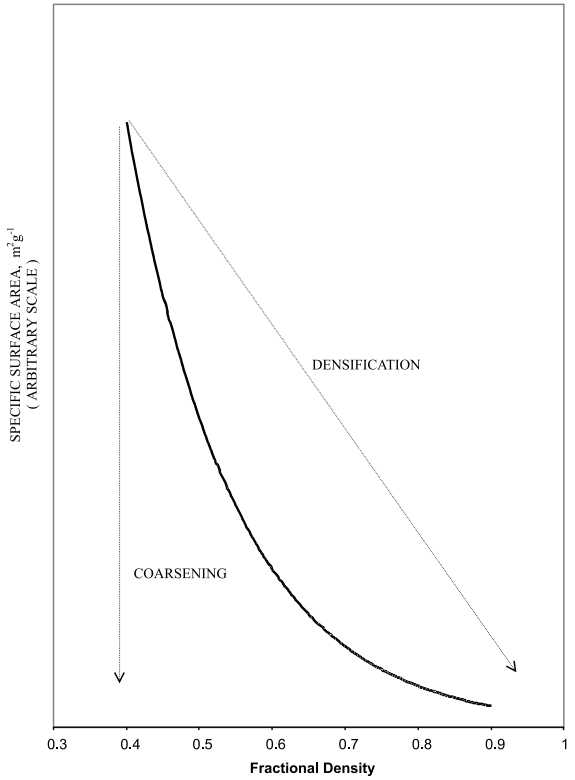

Fig. 3. Variation of specific surface area with increase in density during sintering [33].

Coarsening–densification transition temperature (CDTT) may be defined as the transition temperature between coarsening and densification regimes. One may obtain CDTT for a given material as follows. First, a graph of surface area versus fractional density is drawn. The surface area drops steeply in the coarsening regime but drops little in the densification regime, from which the transition density is noted (Fig. 4). From another graph of sintered density or fractional density versus sintering temperature (Fig. 5), the CDTT can be obtained as that temperature which corresponds to the transition density. In our case, the CDTT works out to be 953°C. Based on CDTT, the sintering furnace profile can be obtained in order to achieve densification.

CDTT is expected to depend on several factors such as the sintering atmosphere, O/U ratio of the compact in the case of a uranium dioxide, green density, particle size, etc. Further, it appears that CDTT decreases as the particle size decreases and as activated sintering increases.

When the particles are loosely packed as in the case of filters there is only coarsening and there is no densification whatever be the heating schedule. Thus, in

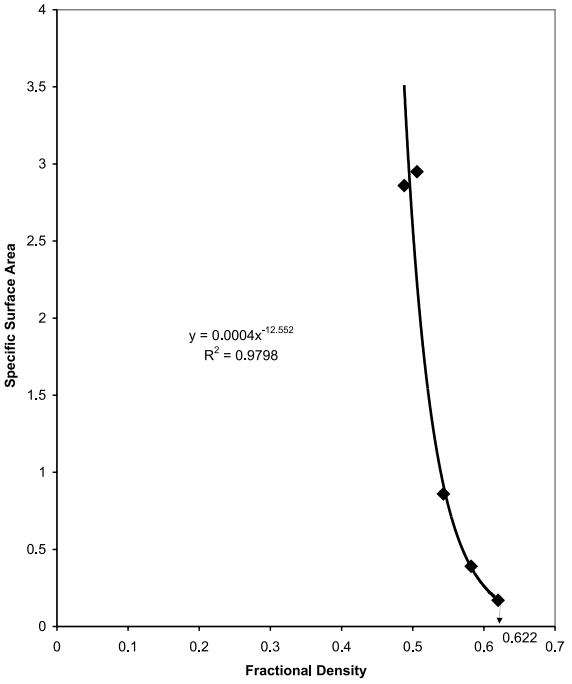

Fig. 4. Fractional density versus specific surface area.

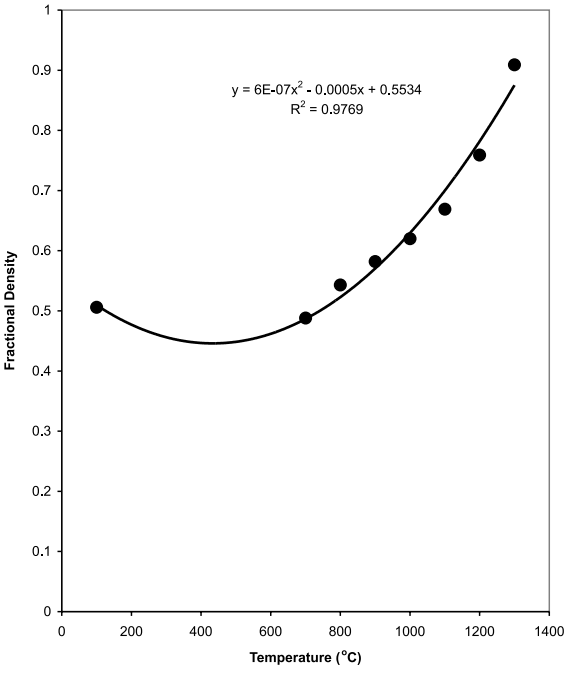

Fig. 5. Fractional density versus sintering temperature.

addition to a low particle size, a high packing efficiency is necessary for achieving densification. If the green microstructure consists of uniformly fine voids between fine particles, even after some coarsening, the reduction in surface energy may not be substantial and densification may still take place at a higher temperature. If the green microstructure is inhomogeneous, substantial reduction in surface energy via coarsening mode affects subsequent densification considerably.

As long as the material is in the coarsening regime, even absence of packing defects cannot help in densification. In the densification regime, the presence of packing defects will inhibit densification and the absence will promote it. Here $p = 2\gamma/r$ is applicable, where p is the sintering pressure, γ is the surface energy, and r is the void radius. Voids less than the critical size will close [34]. The temperature where coarsening ceases and densification starts depends on the particle size. Large particles will not densify even at high temperature.

The coordination number increases as the green density increases. It also increases as sintering proceeds and new contacts between particles develop. The coordination number in the green stage may be further improved by the use of attrited powders [35] and admixed lubricant [36].

Coarsening is aimed at powder preparation where disintegration of the precursor into fine particles is desired. When the powder is being calcined, for the same starting precursor structure, a low temperature of calcination results in fine particles by local surface energy reduction, where particle centers do not approach each other. A high calcination temperature results in large particles [37]. Densification is desired in the sintering of pressed powder compacts but not in powder particles or particle clusters. In sintering of a compact, the surface energy is reduced by densification with particle centers approaching each other in a cooperative manner. While coarsening is desirable in powder particles during calcination, it is undesirable in pressed compact undergoing sintering.

4.2. Phenomenon of coring

Coring in a circular section of a sintered ceramic compact is defined as a core area with a grain size very different from that in the surrounding rim. It is believed to be caused by thermal gradients, additives and differences in particle size. In one type of coring, the grains in the core are larger than those in the rim. Additives or impurities that cause grain growth are present in the core and absent in the rim, probably due to loss during the sintering process. The impurities or additives are soluble in the matrix and cause grain growth by speeding up diffusion. Titania [38,39] and niobia additives are used for achieving large grain size [40] and high density [41] in UO_2 pellets. Coring is associated with discontinuous grain growth and aided by thermal gradients.

In our case, profile N gave coring in some lots and simultaneously the densities were high. The profile was

changed to S and coring disappeared, with a slight lowering of sintered density.

Zawidski et al. [42–44] found that sulfur in UO_2 caused coring when heated at 450°C h^{-1} and there was no coring when the heating rate was reduced to 200°C h^{-1}. The grain size within the core was about 700 μm against 10 μm elsewhere. Even with the slow heating rate of 200°C h^{-1}, the grain size was found to increase from 15 to 90 μm as the sulfur content was increased from 20 to 70 ppm. For thoria-based pellets, Smid [45] stated that trace impurities were removed by vaporization at the pellet exterior, resulting in normal grain growth at the pellet surface and discontinuous grain growth at the pellet interior. Low density in thoria was attributed to the presence of sulfur [46]. In metals, the presence of MnS particles in Fe–3%Si favors the growth of secondary grains [47]. In our case, with the slower heating, the impurity causing coring is believed to have escaped from the compact during the sintering process.

In another type of coring, where the additive is meant for control of grain size, there are large grains in the rim and fine grains in the core. These additives have very little solubility and prevent grain growth by anchoring the grain boundaries and exerting sufficient drag to slow down grain growth. In magnesia-doped alumina, the abnormal grain growth in the rim region was attributed to loss of magnesia from the surface [30].

4.3. Bloating in the lower portion of larger boats

The phenomenon of bloating has been well described in a sintering process [48]. If a gas is trapped in the closed pores its pressure will rise as the pore radius r decreases until it may prevent further shrinkage when an equilibrium condition $p = 2\gamma/r$ is reached, γ being the surface energy. It is energetically favorable from the point of view of energy stored in the compressed gas, and neutral from the point of view of surface energy, for gas to transfer from small pores at high pressure to large pores at low pressure. Such a transfer results in an increase in the total volume of the compact which is termed as 'bloating'. In fact, a theory of kinetics of bloating is described [49] in a relation $r_t^2 - r_0^2 = At$, where r is the radius of pore, t is time, and A is a constant which depends linearly on the solubility of gas and on its diffusion coefficient. Bloating is a result of the pressure exerted by gases from the sintering atmosphere entrapped in large voids in the compact that cannot shrink and close in the course of sintering. It is caused by oversintering of an inhomogeneous green microstructure [50]. UO_2 is usually sintered at about 1700°C in a reducing atmosphere. It is known that UO_2 can be sintered at a lower temperature of 1200°C in mildly oxidizing atmosphere [51] or in the presence of moisture [52]. UO_2 green pellets have excess oxygen which combines with hydrogen to form moisture at about 600°C. The moisture released on the reduction of UO_{2+x} at 600°C is expected to be swept away by the flowing hydrogen gas in the sintering furnace. If the packing of compacts in the boat (charge carrier) is tight, the moisture in the lower portions of the boat may not be able to diffuse out freely and join the flowing gas stream. This accumulated moisture is retained in the boat when it reaches say 1200°C and causes activated sintering. Closure of open porosity occurs at a lower temperature by virtue of the presence of H_2O. As the boat reaches a zone of higher temperature, bloating occurs. Bloating was noticed under profile N only when the charge was doubled and the pellets were close packed, horizontally. There was no bloating under profile S, which allowed time for moisture escape. In vertical loading, where pellets are free standing, there was no bloating even when the charge was large. As there is no contact between the pellets, it is easier for the moisture to move away from the vicinity of the pellets. Bloating can also occur in mixed oxides, when the islands of one constituent dissolve in the matrix, leaving large voids [53].

5. Conclusions

The sintered density of UO_2 is dependent on the heating rate as it determines the residence time of the material in the coarsening and densification regimes of temperature. A coarsening–densification transition temperature has been defined. Presoaking below the CDTT is found to result in lower sintered density, while presoaking above the CDTT is found to result in higher sintered density. The sintering furnace profile or heating rate may be chosen to minimize the time in the low-temperature coarsening regime. By this, the driving force for sintering, namely surface energy reduction, is conserved for availing in densification at a higher temperature in the latter part of sintering.

The adverse or beneficial effect of presoaking on densification may have to be taken into account while considering pretreatments aimed at microstructural refinement. Fast heating rates which result in temperature gradients seem to be favoring densification, but can also sometimes lead to undesirable coring and bloating.

Coring associated with the presence of impurities or additives may be minimized by using a lower heating rate. Bloating in UO_2 may be minimized by ensuring that there is no moisture accumulation near the compacts, by ensuring a slower heating rate, by adequate counter flow of the reducing gas in the sintering furnace, by restricting the quantity of charge in close packed charging or by free-standing arrangement of the compacts.

Acknowledgements

We thank Mr N.P.S. Katiyar and Ms Anuradha for sparing the compaction facility for niobia-doped pellets, Mr H.R. Ravindra for sparing the low-temperature sintering facility and Mr S. Syam Sundar, B. Gopalan and R.B. Yadav for their useful discussions.

References

[1] S.R. Lampman, et al. (Eds.), Ceramics and Glasses, Engineering Materials Handbook, vol. 4, ASM International, Cleveland, OH, 1991.
[2] R.J. Brook (Ed.), Processing of Ceramics, Parts I&II, in: R.W. Cahn, P. Haasen, E.J. Kramer (Eds.), Materials Science and Technology: A Comprehensive Treatment, vols. 17A&B, VCH, New York, 1996.
[3] W.D. Kingery, H.K. Bowen, D.R. Uhlmann, Introduction to Ceramics, 2nd Ed., Wiley, New York, 1976.
[4] J.S. Reed, Introduction to the Principles of Ceramic Processing, Wiley, New York, 1989.
[5] G.Y. Onoda, L.L. Hench (Eds.), Ceramic Processing Before Firing, Wiley, New York, 1978.
[6] D.W. Budworth, An Introduction to Ceramic Science, Pergamon, Oxford, 1970.
[7] R.L. Coble, J.E. Burke, in: J.E. Burke (Ed.), Progress in Ceramic Science, vol. 3, Pergamon, Oxford, 1963, p. 197.
[8] R.M. German, Sintering Theory and Practice, Wiley, New York, 1996.
[9] C. Genuist, J.M. Haussanne, in: J.E. Burke (Ed.), Science of Ceramics, vol. 14, Institute of Ceramics, Shelton, UK, 1988, p. 279.
[10] M.J. Mayo, Int. Mater. Rev. 41 (3) (1996) 85.
[11] A.G. Evans, J. Am. Ceram. Soc. 65 (1982) 497.
[12] R. Raj, R.K. Bordia, Acta Metall. 32 (1984) 1003.
[13] C.H. Hsueh, A.G. Evans, R.M. Cannon, R.J. Brook, Acta Metall. 34 (1986) 1467.
[14] W.H. Juan, E. Gilbart, R.J. Brook, J. Mater. Sci. 24 (1989) 1062.
[15] W.J. Tseng, P.D. Funkenbusch, Physical Chemistry of Powder Metals Production and Processing, The Minerals, Metals and Materials Society, 1989, p. 371.
[16] P. Balakrishna, A. Singh, U.C. Gupta, K.K. Sinha, in: TOP FUEL'97, British Nuclear Energy Society, London (republished in Interceram 48 (1999) 98).
[17] P. Balakrishna, C.K. Asnani, R.M. Kartha, K. Ramachandran, K. Sarat Babu, V. Ravichandran, B. Narasimha Murty, C. Ganguly, Nucl. Technol. 127 (1999) 375.
[18] P. Balakrishna, B. Narasimha Murty, K.P. Chakraborthy, R.N. Jayaraj, C. Ganguly, Mater. Manufact. Process. 15 (2000) 679.
[19] B. Narasimha Murty, P. Balakrishna, R.B. Yadav, C. Ganguly, Powder Technol. 113 (2000) 132.
[20] R. Manzel, W.O. Dorr, Ceram. Bull. 59 (6) (1980) 601,616.
[21] U. Runfors, in: H.H. Hausner (Ed.), Materials and Properties, Modern Developments in Powder Metallurgy, vol. 5, Plenum, New York, 1971, p. 311.
[22] J.L. Woolfrey, J. Am. Ceram. Soc. 55 (1972) 383.
[23] E. Barringer, N. Jubb, B. Fegly, R.L. Pober, H.K. Bowen, in: L.L. Hench, D.D. Ulrich (Eds.), Ultrastructure Processing of Ceramics, Glasses and Composites, Wiley, New York, 1984, p. 315.
[24] M.Y. Chu, L.C. De Jonghe, M.K.F. Lin, F.J.T. Kin, J. Am. Ceram. Soc. 74 (1991) 2902.
[25] E. Sato, C. Carry, J. Eur. Ceram. Soc. 15 (1995) 9.
[26] H. Moon, D.-M. Won, in: Sintering 2000, Belgrade, p. 47.
[27] M. Dondi, M. Marsigli, I. Venturi, Brit. Ceram. Trans. 98 (1) (1999) 12.
[28] A.W. Searcy, D. Beruto, in: D. Taylor (Ed.), Science of Ceramics, vol. 14, Institute of Ceramics, Shelton, UK, 1988, p. 1.
[29] O.J. Whittemore, J.A. Varela, in: G.C. Kuczynski (Ed.), Sintering Processes, Materials Science Research, vol. 13, Plenum, Oxford, 1980, p. 51.
[30] J.E. Burke, J.H. Rosolowski, in: N.B. Hannay (Ed.), Reactivity of Solids, Treatise on Solid State Chemistry, vol. 4, Plenum, New York, 1976, p. 621.
[31] Hj. Matzke, Nonstoichiometric Oxides, Academic, New York, 1981, p. 155.
[32] K. Une, I. Tanabe, M. Oguma, J. Nucl. Mater. 150 (1987) 93.
[33] J.E. Burke, K.W. Lay, S. Prochazka, in: G.C. Kuczynski (Ed.), Sintering Processes, Materials Science Research, vol. 13, Plenum, New York, 1980, p. 417.
[34] T.J. Heal, J.E. Littlechild, R.H. Watson, in: Proceedings of the International Conference on Nuclear Fuel Performance, British Nuclear Energy Society, London, October 15–19, 1973, p. 52.
[35] P. Balakrishna, B. Narasimha Murty, D.V. Ratnam, M. Anuradha, K. Ramachandran, C.K. Asnani, C. Ganguly, Trans. Powder Metall. Assoc. India 26 (1999) 81.
[36] P. Balakrishna, B. Narasimha Murty, R.B. Yadav, M. Anuradha, P.S.A. Narayanan, D. Pramanik, S. Majumdar, Indian J. Eng. Mater. Sci. 5 (1997) 136.
[37] H. Rogan, T.J. Heal, J.E. Littlechild, L.K. Raven, in: Nuclear Fuel Fabrication, Proceedings of the European Nuclear Conference, April 21–25, 1975, Paris, vol. 7, Pergamon, Oxford, 1976, p. 120.
[38] Hj. Matzke, AECL-2585, May 1966.
[39] J.B. Ainscough, F. Rigby, S.C. Osborn, J. Nucl. Mater. 52 (1974) 191.
[40] Y. Harada, J. Nucl. Mater. 238 (1996) 237.
[41] K.W. Song, K.S. Kim, Y.M. Kim, Y.H. Jung, J. Nucl. Mater. 277 (2000) 123.
[42] T.W. Zawidzki, P.S. Apte, M.R. Hoare, J. Am. Ceram. Soc. 67 (5) (1984) 361.
[43] T.W. Zawidzki, P.S. Apte, in: Materials in Nuclear Energy. Proceedings of the International Conference, Huntsville, Ont., 29 September–2 October 1982, American Society for Metals, Cleveland, OH, 1983, p. 68.
[44] T.W. Zawidzki, M.R. Hoare, P.S. Apte, ENL Internal Report, 1978.
[45] R.J. Smid, Am. Ceram. Soc. Bull. 56 (8) (1997) 734 (abstract).
[46] S. Yamagashi, Y. Takahashi, J. Nucl. Mater. 182 (1991) 195.
[47] R.E. Smallman, Modern Physical Metallurgy, Butterworths, London, 1970, p. 399.

[48] M.B. Waldron, B.L. Daniell, in: A.S. Goldberg (Ed.), Monographs in Powder Science and Technology Series, Heyden, London, 1978.
[49] G.W. Greenwood, A. Boltax, J. Nucl. Mater. 5 (1962) 234.
[50] P. Balakrishna, A.P. Kulkarni, T.S. Krishnan, K. Balaramamoorthy, T.R. Ramamohan, P. Ramakrishnan, Advanced Ceramics, Oxford/IBH, New Delhi, 1992, p. 67.
[51] W. Dorr, H. Assmann, in: P. Vincenzini (Ed.), Energy And Ceramics, Materials Science Monograph, vol. 6, Elsevier, Amsterdam, 1980, p. 913.
[52] W.I. Stuart, R.B. Adams, J. Nucl. Mater 58 (1975) 201.
[53] P. Balakrishna, A.P. Kulkarni, G.V.S.R.K. Somayajulu, N. Swaminathan, K. Balaramamoorthy, in: P. Vincenzini (Ed.), Ceramics Today – Tomorrow's Ceramics, Materials Science Monograph, vol. 66D, Elsevier, Amsterdam, 1991, p. 3003.